

Parasitic Momentum Flux in the Tokamak Core

T. Stoltzfus-Dueck¹

Princeton University, Princeton, NJ 08544^{a)}

(Dated: November 29, 2016)

A geometrical correction to the $\mathbf{E} \times \mathbf{B}$ drift causes an outward flux of cocurrent momentum whenever electrostatic potential energy is transferred to ion parallel flows. The robust symmetry breaking follows from the free energy flow in phase space and does not depend on any assumed linear eigenmode structure, acting both for axisymmetric fluctuations (such as geodesic acoustic modes) as well as more general nonaxisymmetric fluctuations. The resulting rotation peaking is countercurrent and scales as electron temperature over plasma current. This peaking mechanism can only act when fluctuations are low-frequency enough to excite ion parallel flows, which may explain some recent experimental observations related to rotation reversals.

PACS numbers: 52.25.Dg, 52.25.Fi, 52.25.Xz, 52.30.Gz, 52.35.We, 52.55.Dy, 52.55.Fa

Keywords: toroidal rotation, tokamak, transport, intrinsic rotation, rotation reversal

Tokamak plasmas without applied torque routinely rotate spontaneously in the toroidal (symmetry) direction, exhibiting nonzero, sheared toroidal rotation profiles.¹ This so-called “intrinsic” rotation is not only of fundamental interest: toroidal rotation helps suppress certain instabilities² and its shear may reduce turbulent heat transport.³ These advantages are important for future burning plasma devices such as ITER, in which the dominant α -heating will not exert toroidal torque, unlike the neutral beam heating typical of present-day devices.⁴

Although experimentally measured intrinsic rotation profiles are very diverse, many exhibit three distinct radial regions: an edge region with cocurrent rotation (toroidal rotation in the direction of the plasma current I_p), a mid-radius “gradient region” where rotation either becomes increasingly countercurrent with decreasing radius (countercurrent peaking) or stays relatively flat, and a flat or weakly cocurrent-peaked central region affected by sawtoothing.^{5–9} Previous theoretical,¹⁰ numerical,¹¹ and experimental⁶ work suggests that the edge rotation is driven by the interaction of passing-ion drift orbit excursions with spatial variation of the turbulent fluctuations. The present work focuses on the “gradient region” at intermediate radius, where radial variation of plasma parameters is much slower, allowing other effects to compete with those of orbit excursions.

Over the last decade, intrinsic rotation at mid-radius has undergone intense theoretical and experimental investigation. Nonaxisymmetric magnetic fields can strongly affect the toroidal rotation.¹² The present work will focus exclusively on the case of axisymmetric confining magnetic field, for which the conservation of toroidal angular momentum¹³ excludes the possibility of a self-generated torque. Intrinsic rotation must therefore result from a nondiffusive component to the momentum flux. Neoclassical (collisional) momentum fluxes are much too small to explain experimental observations, implying that turbulent transport is dominant.¹ A number

of turbulent calculations suggest the presence of a momentum pinch, a component of momentum flux that is proportional to the toroidal rotation itself, rather than its gradient.¹⁴ However, these models cannot explain the common observation of sheared velocity profiles passing through zero.^{5–9} Such measurements imply the presence of a “residual stress,” meaning a momentum flux contribution that is independent of both toroidal rotation and its radial gradient. For up-down symmetric geometries, often a good approximation for tokamak core plasmas, symmetry arguments restrict the leading-order momentum flux terms from driving residual stress.¹⁵ Theoretical work has accordingly focused on symmetry-breaking mechanisms¹⁵ such as $\mathbf{E} \times \mathbf{B}$ shear,¹⁶ up-down-asymmetric geometry,¹⁷ and polarization effects.¹⁸ Particularly challenging to theory are the experimental observations of rotation reversals in the “gradient region,” in which countercurrent rotation peaking suddenly flattens or switches to weak cocurrent peaking when plasma density or current cross threshold values.^{7–9} The rapidity of these reversals suggests that the direction of peaking is not determined by neoclassical flows or other quantities that vary smoothly with plasma parameters, following instead from the properties of the turbulence itself, which may suddenly change character e.g. as an instability threshold is crossed. In this letter, I identify a geometrical correction to the $\mathbf{E} \times \mathbf{B}$ drift, neglected in all previous analytical work, that causes the free energy flows within the turbulence to drive a robust, fully nonlinear symmetry-breaking momentum flux. This flux causes counter-current core rotation peaking consistent with experimental measurements, and explains several observations related to rotation reversals.

To develop intuition, consider first a low-frequency axisymmetric density perturbation, as sketched in Fig. 1. At low frequencies and large scales, electron parallel force balance ensures that the nonzonal electrostatic potential $\tilde{\phi}$ is proportional to the nonzonal ion gyrocenter density \tilde{n}_i . The pressure gradient and electric field then cause ions to flow out of the dense region along the magnetic field. The poloidal electric field also causes a radial $\mathbf{E} \times \mathbf{B}$ drift that advects counter- (co-)current ion momentum

^{a)} Electronic mail: tstoltzf@princeton.edu

inward (outward), regardless of the signs of I_p and the toroidal magnetic field B_T .

Key to this mechanism is a dual role for the weak electric field caused by the poloidal variation of the potential ϕ on length scales comparable to the minor radius r . The nonvanishing parallel component of this electric field allows it to cause local ion acceleration, resulting in energy transfer between electrostatic potential (ϕ) and parallel ion flow ($u_{\parallel i}$). Because the background plasma gradients predominantly supply energy to even moments of the distribution function (such as density), while odd moments (such as $u_{\parallel i}$) are subjected to dissipation,^{19,20} steady-state energy balance often requires a net transfer of free energy from the potential (a function of even moments) to the ion parallel flows, causing a statistical symmetry breaking in the corresponding energy transfer term. Although toroidal angular momentum conservation does not allow the self-generated electric field to impart a net torque to the plasma, the weak radial $\mathbf{E} \times \mathbf{B}$ drift due to the poloidally varying ϕ may transport toroidal angular momentum in the radial direction. The correlations between the ion parallel flows and the weak radial $\mathbf{E} \times \mathbf{B}$ drift, resulting from the statistical symmetry breaking due to energy transfer, cause this part of the momentum flux to have a preferred sign, independent of plasma rotation and its radial gradient. In this letter, we will consider this residual stress in two separate cases: first a simpler special case with axisymmetric fluctuations, where the momentum flux occurs due to damping of geodesic acoustic modes (GAMs) via ion parallel flows, and later a more general case including nonaxisymmetric fluctuations, where the momentum flux can occur for any turbulent fluctuations in which energy transfer from potential to ion parallel flow is nonnegligible.

Both calculations use the simplest model capturing the relevant physics: the large-aspect-ratio limit of the electrostatic, isothermal gyrofluid equations in a radially thin geometry,^{19,21} written in cgs units as

$$\partial_t n_s + \mathbf{u}_{Es} \cdot \nabla (n_s + n_{s0}) = \mathcal{K} \left(\frac{n_s T_{s0}}{Ze} + n_{s0} \phi_G \right) - n_{s0} \nabla_{\parallel} u_{\parallel s}, \quad (1)$$

$$m_s n_{s0} (\partial_t + \mathbf{u}_{Es} \cdot \nabla) u_{\parallel s} = -\nabla_{\parallel} (n_s T_{s0} + Ze n_{s0} \phi_G) + m_s n_{s0} \left[\frac{2}{Ze} T_{s0} \mathcal{K}(u_{\parallel s}) - D_{\parallel s} \right], \quad (2)$$

$$\sum_s n_{s0} Z^2 e^2 \frac{1 - \Gamma_{0s}}{T_{s0}} \phi = \sum_s Ze \Gamma_{1s} n_s, \quad (3)$$

with species subscript s meaning ions i or electrons e ; species charge state Z (-1 for electrons), mass m_s , and (constant) temperature T_{s0} ; fluctuating n_s and equilibrium n_{s0} species density (assuming $Zn_{i0} = n_{e0}$); $\mathbf{E} \times \mathbf{B}$ drift $\mathbf{u}_{Es} \doteq (c/B)\hat{\mathbf{b}} \times \nabla \phi_G$; gyroaveraged potential $\phi_G \doteq \Gamma_{1s} \phi$; curvature operator $\mathcal{K} \doteq -(2c/B)\hat{\mathbf{b}} \times \nabla \ln B \cdot \nabla$ capturing the magnetic drifts and $\mathbf{E} \times \mathbf{B}$ divergence; parallel gradient $\nabla_{\parallel} \doteq \hat{\mathbf{b}} \cdot \nabla$; parallel flow velocity $u_{\parallel s}$; and dissipation operator $D_{\parallel s}$. The gyroaveraging operators Γ_{0s} and Γ_{1s} take the low- k_{\perp} limits $(1 - \Gamma_{0s}) \rightarrow -\rho_s^2 \nabla_{\perp}^2$ and $\Gamma_{1s} \rightarrow 1$, for $\rho_s = v_{ts}/|\Omega_{cs}|$ the species gyroradius,

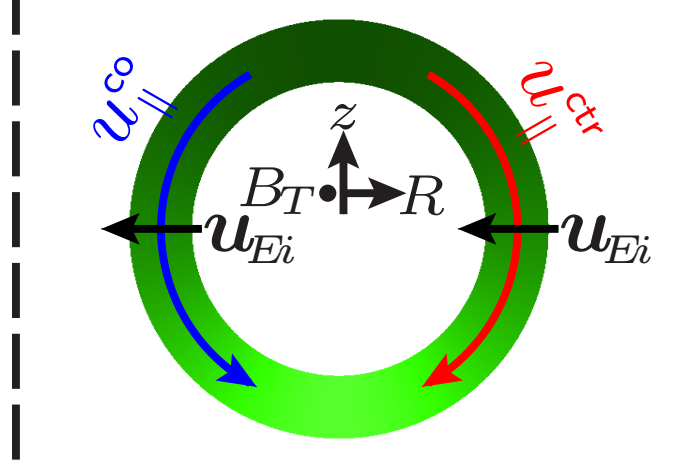


Figure 1. Poloidal cut of a low-frequency axisymmetric fluctuation, with axis of symmetry on the left. Darker shading shows larger \tilde{n}_i , proportional to $\tilde{\phi}$ by the low- k_{\perp} electron adiabatic response. Given enough time, ions flow out of the dense region along the magnetic field, causing counter-current (red) toroidal flow toward decreasing θ and co-current (blue) toward increasing θ . The poloidal variation of $\tilde{\phi}$ causes an $\mathbf{E} \times \mathbf{B}$ flow that is inward for the counter-current ion flux and outward for the cocurrent flux. Reversing the toroidal magnetic field switches the poloidal direction of counter- and cocurrent flow as well as the sign of the $\mathbf{E} \times \mathbf{B}$ drift \mathbf{u}_{Ei} , leaving the momentum flux unchanged. The poloidal orientation of the density perturbation has no effect on the sign or magnitude of this momentum flux.

with thermal speed $v_{ts} \doteq (T_{s0}/m_s)^{1/2}$ and gyrofrequency $\Omega_{cs} \doteq ZeB_0/m_sc$. We take safety factor $q = B_T r/B_p R_0$ order unity, so the poloidal field and inverse aspect ratio are comparably small, $B_p/B_T \sim r/R_0 \ll 1$, allowing explicit appearances of B and R to be replaced with representative constants B_0 and R_0 , and setting $b_T \doteq \hat{\mathbf{b}} \cdot \hat{\mathbf{z}} \rightarrow \pm 1$ for magnetic and toroidal directions $\hat{\mathbf{b}}$ and $\hat{\mathbf{z}}$. Since the toroidal component of \mathbf{u}_{Es} is small in B_p/B_T , Eqs. (1)–(3) conserve a simplified toroidal angular momentum involving only the zonal (flux-surface) average $\langle \dots \rangle$ of $u_{\parallel i}$, assuming $\langle D_{\parallel i} \rangle = 0$:

$$\partial_t \langle L_{\zeta} \rangle = -\partial_x \langle \Pi_{\zeta} \rangle, \quad (4)$$

with toroidal angular momentum density and flux $L_{\zeta} \doteq m_i n_{i0} b_T R_0 u_{\parallel i}$, $\Pi_{\zeta} \doteq m_i n_{i0} b_T R_0 (u_{Ei}^x - \frac{2T_{i0}}{Ze} \mathcal{K}^x) u_{\parallel i}$, with $u_{Ei}^x \doteq \mathbf{u}_{Ei} \cdot \nabla x$, $\mathcal{K}^x \doteq \mathcal{K}(x)$, and radial (flux-surface) label x . Eq. (4) shows that toroidal angular momentum is advected by the $\mathbf{E} \times \mathbf{B}$ and magnetic drifts, without sources or sinks.

A nondiffusive momentum flux as in Fig. 1 may be driven by geodesic acoustic mode (GAM) damping, which we may treat in a shearless simple-circular geometry, $\mathcal{K}^x \rightarrow (2cb_T/B_0 R_0) \sin \theta$ for poloidal angle θ . Following Ref. 22, we retain only one axisymmetric Fourier component from each of Eqs. (1)–(3), specifically $n_i^s \doteq \langle n_i \sin \theta \rangle$, $u_{\parallel}^c \doteq \langle u_{\parallel i} \cos \theta \rangle$, and $u_E^z \doteq \langle u_{Ei} \theta \rangle$ with

$u_{Ei} \doteq \mathbf{u}_{Ei} \cdot \hat{\theta} = b_T \frac{c}{B_0} \partial_x \phi$. We neglect electron polarization and take low- k_\perp gyroaveraging and quasineutrality $Z \langle n_i \sin \theta \rangle \approx \langle n_e \sin \theta \rangle$, and electron adiabatic response $T_{e0} \langle n_e \sin \theta \rangle \approx en_{e0} \langle \phi \sin \theta \rangle$, obtaining

$$\partial_t n_i^s = n_{i0} u_E^z / R_0 + b_p n_{i0} u_\parallel^c / r - \partial_x \langle \Gamma_i \sin \theta \rangle, \quad (5)$$

$$m_i n_{i0} \partial_t u_\parallel^c = -b_p T_a n_i^s / r - \nu_\parallel m_i n_{i0} u_\parallel^c - \partial_x \langle \Pi_\parallel \cos \theta \rangle, \quad (6)$$

$$n_{i0} m_i \partial_t u_E^z = -2T_a n_i^s / R_0 - \partial_x \langle \Pi_E \rangle, \quad (7)$$

in which $b_p \doteq \hat{b} \cdot \hat{\theta} \ll 1$ and $T_a \doteq T_{i0} + ZT_{e0}$. We have taken $\langle D_{\parallel i} \cos \theta \rangle \rightarrow \nu_\parallel u_\parallel^c$ for parallel flow damping rate ν_\parallel . The Γ_i , Π_\parallel , and Π_E terms respectively capture the divergences of ion density, parallel/toroidal momentum, and $\mathbf{E} \times \mathbf{B}$ /poloidal momentum fluxes due to unresolved Fourier components. The $\partial_x \langle \Pi_E \rangle$ form follows from Eq. (3), with $\Pi_E \approx m_i n_{i0} u_{Ei\theta} u_{Ei}^z$ plus FLR corrections.¹³ Linearizing Eqs. (5)–(7) and neglecting Γ_i , Π_\parallel , and Π_E yields a simple dispersion relation

$$\omega^2 - 2 \frac{T_a}{m_i R_0^2} = \frac{\omega}{\omega + i\nu_\parallel} \frac{T_a}{m_i q^2 R_0^2}. \quad (8)$$

For $q \gg 1$, Eq. (8) contains a pair of weakly damped high-frequency GAMs $\omega \approx \pm (2T_a/m_i R_0^2)^{1/2} - i\nu_\parallel/4q^2$. However, for q near 1, as is typical in tokamak core plasmas, the GAMs damp at a significant fraction of $\nu_\parallel \sim v_{ti}/qR$, as seen in more detailed kinetic calculations.²³

To evaluate and physically understand the resulting toroidal momentum flux, we examine the free energy balance for n_i^s , u_\parallel^c , and u_E^z :

$$\partial_t E_i^s = 2T_a n_i^s [u_E^z / R_0 + b_p u_\parallel^c / r - n_{i0}^{-1} \partial_x \langle \Gamma_i \sin \theta \rangle], \quad (9)$$

$$\partial_t E_\parallel^c = -2u_\parallel^c (b_p T_a n_i^s / r + \nu_\parallel m_i n_{i0} u_\parallel^c + \partial_x \langle \Pi_\parallel \cos \theta \rangle), \quad (10)$$

$$\partial_t E_E^z = -2T_a n_i^s u_E^z / R_0 - u_E^z \partial_x \langle \Pi_E \rangle, \quad (11)$$

in which $E_i^s \doteq T_a (n_i^s)^2 / n_{i0}$, $E_\parallel^c \doteq m_i n_{i0} (u_\parallel^c)^2$, and $E_E^z \doteq \frac{1}{2} n_{i0} m_i (u_E^z)^2$. Turbulence simulations show that the Reynolds stress (Π_E) typically acts as a source for E_E^z , the geodesic transfer term ($\propto n_i^s u_E^z$) moves free energy from E_E^z to E_i^s , and both parallel flow excitation ($\propto n_i^s u_\parallel^c$) and the turbulent density flux sideband ($\propto \partial_x \langle \Gamma_i \sin \theta \rangle$) move energy out of E_i^s .^{22,24} Note next that the electron adiabatic response combined with nonzero n_i^s implies a radial $\mathbf{E} \times \mathbf{B}$ drift $\langle u_{Ei}^x \cos \theta \rangle = -cb_T \langle \phi \sin \theta \rangle / Br = -cb_T T_{e0} n_i^s / en_{i0} Br$. Recalling Eq. (4), this beats with u_\parallel^c to cause a contribution $\Pi_\zeta^{(G)} = -2(ZT_{e0}/T_{i0})(\rho_i/r)m_i R_0 v_{ti} n_i^s u_\parallel^c$ to the toroidal angular momentum flux $\langle \Pi_\zeta \rangle$. Since $\Pi_\zeta^{(G)}$ is directly proportional to the parallel flow excitation term in Eqs. (9) and (10), we conclude that energy transfer from the pressure sideband to the parallel ion flow necessarily implies an outflux of cocurrent toroidal angular momentum. Indeed, since the turbulent flux term $-2u_\parallel^c \partial_x \langle \Pi_\parallel \cos \theta \rangle$ will typically transfer energy out of E_\parallel^c , we may use the statistical average $\overline{\cdots}$ of Eq. (10), $-b_p T_a \overline{n_i^s u_\parallel^c} / r \gtrsim \nu_\parallel m_i n_{i0} \overline{(u_\parallel^c)^2}$, to

conservatively estimate the (signed) momentum flux as $\Pi_\zeta^{(G)} \sim 2(\nu_\parallel/b_p \Omega_{ci})(ZT_{e0}/T_a)n_{i0}m_i R_0 \overline{(u_\parallel^c)^2}$. Although simple ordering estimates suggest this flux may only drive toroidal ion thermal Mach numbers of order (ρ_i/r) times the ratio of GAM kinetic energy over turbulent fluctuations' kinetic energy, its fixed relation to the free-energy transfer guarantees robust symmetry breaking whenever there is strong GAM damping acting via ion parallel flows. Quantitative evaluation of its magnitude will require numerical simulation.

What is happening here physically? First, Reynolds stress excites a poloidal $\mathbf{E} \times \mathbf{B}$ flow. Poloidal variation of B causes a divergence in the $\mathbf{E} \times \mathbf{B}$ velocity, resulting in up-down-asymmetric density fluctuations, like those sketched in Fig. 1. The resulting poloidal electric field (due to adiabatic electron response) and ion pressure gradient jointly excite an ion flow along \mathbf{B} . The net energy flow from Reynolds stress drive to damping via the ion parallel flow implies a positive correlation of the poloidal electric field and poloidal ion flow. The poloidal electric field also causes a weak radial $\mathbf{E} \times \mathbf{B}$ drift. Due to the pitch of the magnetic field, the poloidal ion flow along the field corresponds to co- (counter-)current toroidal flow where the $\mathbf{E} \times \mathbf{B}$ drift points radially outward (inward), which causes counter-current rotation peaking.

Energy transfer from nonaxisymmetric potential fluctuations to ion parallel flows can drive an even stronger toroidal momentum flux, but in order to understand its origin we must first discuss the field-aligned magnetic coordinates used in most gyrokinetic formulations: Consider now an axisymmetric geometry with good nested flux surfaces, but otherwise arbitrary. Radial position is specified by a flux-surface label ρ , which is axisymmetric and satisfies $\hat{b} \cdot \nabla \rho = 0$. Poloidal position is specified by a distended but axisymmetric poloidal angle label ϑ . The third coordinate ξ is chosen so that $\hat{b} \cdot \nabla \xi = 0$, letting it label perpendicular position within the flux surface. These choices are not arbitrary: The definition of ξ implies that $\hat{b} \cdot \nabla = (\hat{b} \cdot \nabla \vartheta) \partial_\vartheta$ so $\partial_\vartheta|_{\rho, \xi} = (\hat{b} \cdot \nabla \vartheta)^{-1} \hat{b} \cdot \nabla$ contains only slow variation. The use of an axisymmetric ρ and ϑ implies that the partial $\partial_\xi|_{\rho, \vartheta}$ is proportional to a simple toroidal derivative $\hat{\zeta} \cdot \nabla$, since holding ρ and ϑ fixed is equivalent to holding R and vertical position z fixed. This property has two important implications. First, appropriate choice of ξ allows toroidal periodicity to imply simple periodicity in ξ . Second, $\partial_\xi \propto \hat{\zeta} \cdot \nabla$ vanishes for any axisymmetric quantity, in particular for equilibrium plasma parameters and the magnetic geometry. These properties allow one to construct symmetry arguments that the dominant toroidal angular momentum flux, due to the $\partial_\xi \phi$ portion of \mathbf{u}_{Ei} , must vanish in the statistical average for leading-order local gyrokinetic formulations with up-down symmetric magnetic geometry.¹⁵ In contrast, the $\partial_\vartheta \phi$ portion of \mathbf{u}_{Ei} , neglected in all previous analytical works, is unrestricted by the symmetry arguments¹⁵ and indeed must break symmetry in the (common) case of net energy transfer from ϕ to ion parallel flows, as we will derive now.

any radially global effects. Although $\Pi_{\zeta}^{(2)}$ results from a higher-order part of the $\mathbf{E} \times \mathbf{B}$ drift ($\mathbf{u}_{Ei}^{(2)}$), which should have little direct impact on the leading-order turbulence, it is slaved to free energy fluxes that are determined by the leading-order physics. It can therefore be estimated even by simulations that neglect $\mathbf{u}_{Ei}^{(2)}$, simply by evaluating the relevant energy flux term *a posteriori*.

Although quantitative evaluation requires nonlinear simulation, we may qualitatively compare $\Pi_{\zeta}^{(2)}$ with experimental rotation observations. The general scaling for the countercurrent velocity peaking (roughly the toroidal velocity at the $q = 1$ surface minus that at the pedestal top) is $f_L(ZT_{e0}/T_{i0})(\rho_{i0}/L_p)v_{ti} \approx 5f_L[T_{e0}(\text{keV})/I_p(\text{MA})](r/L_p)\text{km/s}$, which resembles Rice scaling ($\propto 1/I_p$) and has a magnitude comparable with experimental observations.⁵⁻⁸ Also, in ASDEX-Upgrade (AUG), countercurrent momentum peaking has correlated strongly with density peaking across many discharge types.⁸ The relation may be more coincidental than causal: density peaking tends to occur due to electron precessional resonance for fluctuations with $\omega \lesssim v_{ti}/R$,²⁶ which (at core $q \sim 1$) are the same modes that can excite ion parallel flows, thus driving countercurrent peaking. Interestingly, on Alcator C-mod, the presence of countercurrent peaking is correlated with the disappearance of broadband high- k_{\perp} density fluctuations.⁷ Viewed theoretically, dominant dissipation via low- k_{\perp} ion parallel flows, which implies countercurrent rotation peaking in the present model, would also imply the reduction or elimination of a strong direct cascade of density fluctuations to high k_{\perp} , consistent with C-mod measurements. Further qualitative and quantitative comparisons are needed.

In conclusion, a geometrical correction to the $\mathbf{E} \times \mathbf{B}$ drift causes an outward flux of cocurrent momentum whenever electrostatic potential energy is transferred to ion parallel flows. The robust symmetry breaking follows from the free energy flow in phase space and does not depend on assumed linear eigenmode structure. The resulting rotation peaking is countercurrent and scales with $(ZT_{e0}/T_{i0})(\rho_{i0}/L_p)v_{ti} \propto (T_{e0}/I_p)(r/L_p)$. This peaking mechanism can only act when fluctuations are low-frequency enough to excite ion parallel flows, which may explain some recent experimental observations.^{7,8}

Helpful discussions with C. Angioni, G. Hammett, P. Helander, J. Krommes, and B. Scott, and funding by the Max-Planck/Princeton Center for Plasma Physics are gratefully acknowledged.

¹J. S. deGrassie, Plasma Phys. Controlled Fusion **51**, 124047 (2009).

²E. Strait, T. S. Taylor, A. D. Turnbull, J. R. Ferron, L. L. Lao, B. Rice, O. Sauter, S. J. Thompson, and D. Wróblewski, Phys. Rev. Lett. **74**, 2483 (1995).

³H. Biglari, P. H. Diamond, and P. W. Terry, Phys. Fluids B **2**, 1 (1990).

⁴E. J. Doyle, W. A. Houlberg, Y. Kamada, V. Mukhovatov, T. H. Osborne, A. Polevoi, G. Bateman, J. W. Connor, J. G. Cordey, T. Fujita, *et al.*, Nucl. Fusion **47**, S18 (2007).

⁵J. S. deGrassie, J. E. Rice, K. H. Burrell, R. J. Groebner, and W. M. Solomon, Phys. Plasmas **14**, 056115 (2007); L.-G. Eriksson, T. Hellsten, M. F. F. Nave, J. Brzozowski, K. Holmström, T. Johnson, J. Ongena, K.-D. Zastrow, and JET-EFDA Contributors, Plasma Phys. Controlled Fusion **51**, 044008 (2009); R. M. McDermott, C. Angioni, R. Dux, E. Fable, T. Pütterich, F. Rytter, A. Salmi, T. Tala, G. Tardini, E. Viezzer, and the ASDEX Upgrade Team, *ibid.* **53**, 124013 (2011).

⁶T. Stoltzfus-Dueck, A. N. Karpushov, O. Sauter, B. P. Duval, B. Labit, H. Reimerdes, W. A. J. Vijvers, Y. Camenen, and the TCV Team, Phys. Rev. Lett. **114**, 245001 (2015); Phys. Plasmas **22**, 056118 (2015).

⁷J. E. Rice, B. P. Duval, M. L. Reinke, Y. A. Podpaly, A. Bortolon, R. M. Churchill, I. Cziegler, P. H. Diamond, A. Dominguez, P. C. Ennever, *et al.*, Nucl. Fusion **51**, 083005 (2011).

⁸C. Angioni, R. M. McDermott, F. J. Casson, E. Fable, A. Botino, R. Dux, R. Fischer, Y. Podoba, T. Pütterich, F. Rytter, E. Viezzer, and ASDEX Upgrade Team, Phys. Rev. Lett. **107**, 215003 (2011).

⁹O. Sauter, B. P. Duval, L. Federspiel, F. Felici, T. P. Goodman, A. Karpushov, S. Puddu, J. Rossel, and the TCV team, in *Fusion Energy Conference 2010 Book of Abstracts* (IAEA, 2010) p. 180.

¹⁰T. Stoltzfus-Dueck, Phys. Rev. Lett. **108**, 065002 (2012); Phys. Plasmas **19**, 055908 (2012).

¹¹J. Seo, C. S. Chang, S. Ku, J. M. Kwon, W. Choe, and S. H. Müller, Phys. Plasmas **21**, 092501 (2014).

¹²J.-K. Park, Y. M. Jeon, J. E. Menard, W. H. Ko, S. G. Lee, Y. S. Bae, M. Joung, K.-I. You, K.-D. Lee, N. Logan, *et al.*, Phys. Rev. Lett. **111**, 095002 (2013).

¹³B. Scott and J. Smirnov, Phys. Plasmas **17**, 112302 (2010); A. J. Brizard and N. Tronko, **18**, 082307 (2011).

¹⁴T. S. Hahm, P. H. Diamond, O. D. Gurcan, and G. Rewoldt, Phys. Plasmas **14**, 072302 (2007); A. G. Peeters, C. Angioni, Y. Camenen, F. J. Casson, W. A. Hornsby, A. P. Snodin, and D. Strintzi, **16**, 062311 (2009).

¹⁵A. G. Peeters, C. Angioni, A. Bortolon, Y. Camenen, F. J. Casson, B. Duval, L. Fiederspiel, W. A. Hornsby, Y. Idomura, T. Hein, *et al.*, Nucl. Fusion **51**, 094027 (2011).

¹⁶R. R. Dominguez and G. M. Staebler, Phys. Fluids B **5**, 3876 (1993).

¹⁷Y. Camenen, A. G. Peeters, C. Angioni, F. J. Casson, W. A. Hornsby, A. P. Snodin, and D. Strintzi, Phys. Rev. Lett. **102**, 125001 (2009).

¹⁸C. J. McDermott, P. H. Diamond, Ö. D. Gürcan, and T. S. Hahm, Phys. Plasmas **16**, 052302 (2009).

¹⁹B. Scott, Phys. Plasmas **17**, 102306 (2010).

²⁰T. Stoltzfus-Dueck, In preparation.

²¹B. D. Scott, Plasma Phys. Controlled Fusion **45**, A385 (2003).

²²B. D. Scott, New J. Phys. **7**, 92 (2005).

²³S. V. Novakovskii, C. S. Liu, R. Z. Sagdeev, and M. N. Rosenbluth, Phys. Plasmas **4**, 4272 (1997); H. Sugama and T.-H. Watanabe, J. Plasma Phys. **72**, 825 (2006); **74**, 139 (2008).

²⁴N. Miyato, Y. Kishimoto, and J. Li, Phys. Plasmas **11**, 5557 (2004).

²⁵For an atypical case with inverse ion Landau damping, meaning energy transfer from $E_{\parallel i}$ to E_E , $\Pi_{\zeta}^{(2)}$ would reverse sign and cause cocurrent peaking.

²⁶C. Angioni, Y. Camenen, F. J. Casson, E. Fable, R. M. McDermott, A. G. Peeters, and J. E. Rice, Nucl. Fusion **52**, 114003 (2012).